Reactive spark plasma sintering of Ti3SnC2, Zr3SnC2 and Hf3SnC2 using Fe, Co or Ni additives

Thomas Lapauw, Bensu Tunca, Thierry Cabioc'h, Jozef Vleugels, Konstantina Lambrinou

Submitted version

Reactive Spark Plasma Sintering of Ti_3SnC_2, Zr_3SnC_2 and Hf_3SnC_2 using Fe, Co or Ni additives

Authors

Thomas Lapauw[a,b*], Bensu Tunca[a,b], Thierry Cabioc'h[c], Jozef Vleugels[a] and Konstantina Lambrinou[b,c]

[a] KU Leuven, Department of Materials Engineering, Kasteelpark Arenberg 44, B-3001 Leuven, Belgium

[b] SCK•CEN, Boeretang 200, B-2400 Mol, Belgium

[c] Institut Pprime, UPR 3346, Université de Poitiers-ENSMA, SP2MI, Téléport 2-BP 30179, 86962 Futuroscope Chasseneuil Cedex, France

* Corresponding author. Address: KU Leuven, Department of Materials Engineering, Kasteelpark Arenberg 44, B-3001 Leuven, Belgium. Tel.: + 32 16 37 36 05; fax: + 32 16 32 19 90

E-mail address: thomas.lapauw@kuleuven.be (T. Lapauw)

Keywords

MAX phase; spark plasma sintering; X-ray diffraction

Abstract

This work studied the effect of adding 10 at% Fe, Co or Ni to M-Sn-C mixtures with M = Ti, Zr or Hf on MAX phases synthesis by reactive spark plasma sintering. Adding Fe, Co or Ni assisted the formation of 312 MAX phases, i.e., Ti_3SnC_2, Zr_3SnC_2 and Hf_3SnC_2, while their 211 counterparts Ti_2SnC, Zr_2SnC and Hf_2SnC formed in the undoped M-Sn-C mixtures. The lattice parameters of the newly synthesized Zr_3SnC_2 and Hf_3SnC_2 MAX phases were determined by X-ray diffraction. Binary MC carbides were present in all ceramics, whereas the formation of intermetallics was largely determined by the selected additive. The effect of adding Fe, Co or Ni on the MAX phase crystal structure and the microstructure of the produced ceramics was investigated in greater detail for the case of M = Zr. A mechanism is herein proposed for the formation of M_3SnC_2 MAX phases.

Introduction

A wide variety of ternary carbide and nitride materials were investigated in the 1960s. A set of these complex carbides and nitrides was designated H-phases with Cr_2AlC as stereotypic crystal structure [1, 2]. Apart from the performed crystallographic investigation, limited information was provided on the macroscopic properties of these hexagonal structures. In the 1990s, Barsoum et al. purified Ti_3SiC_2, which is structurally related to the Cr_2AlC-type phases [3, 4]. These authors observed remarkable properties, some of which are characteristic of ceramics and some of metals, since these materials demonstrate chemical and thermal stability, good electrical and thermal conductivity, elastic stiffness, and damage tolerance due to particular energy-absorbing mechanisms (delamination, crack bridging, etc.). This behavior is associated with the nano-laminated crystal structure of these carbides and nitrides, described by the general formula $M_{n+1}AX_n$, where 'M' is an early transition metal, 'A' is an element from group 13,14 or 15 in the periodic table, 'X' is C or N, and 'n' is an integer commonly taking the value 1, 2 or 3 and determining how many octahedrons separate the A-group element layers. The subtypes determined by the 'n' value are referred to as 211, 312 or 413 structures. This alternation of n-M_6X octahedrons with A-layers is the key behind the observed extraordinary behavior that is the driving force behind MAX phase research for the last 20 years [3-5]. The broad variety of M and A elements, the various 'n' values and, particularly, the elemental interchangeability on the M and A sites that results in quaternary or even more complex solid solutions or ordered structures, increase the possible members of the MAX phase family exponentially [6, 7].

Considering the reported ternary phases, new stable combinations of M, A and X are still being discovered. Some of the most recently-discovered ternary MAX phases are Mn_2GaC, Zr_2AlC, Zr_3AlC_2, Hf_2AlC, Hf_3AlC_2, Ti_3AuC_2 and Ti_3IrC_2 [8-12]. New MAX structures are also found for existing ternary combinations by observing different atomic stackings (typical for higher 'n' values), as in the case of Ti_3InC_2, Ti_3GaC_2 and Ti_3SnC_2 [13, 14]. Considering Ti_3SnC_2, the presence of Fe, either from the hot isostatic pressing (HIP) capsule or in the starting powder, is essential to form the 312 structure [14, 15]. The other reported Sn-containing MAX phases are all 211 structures, i.e., Ti_2SnC, Zr_2SnC, Hf_2SnC and Nb_2SnC [2, 16]. Jeitschko et al. reported the unsuccessful attempt to synthesize Ta_2SnC, even after very long heat-treatments [17].

The interest in new Sn-containing MAX phases is twofold. First, a recent study reported the crack-healing behavior of Ti_2SnC after oxidation that restored the material's mechanical strength close to the room temperature value [18]. Second, Zr_2SnC is one of the few near phase-pure Zr-containing MAX phases ever reported [16]. MAX phases with Zr as M element are of interest for the nuclear industry, as Zr has a small neutron cross-section, making them attractive candidates materials for fuel cladding applications. Considering the synthesis technique, spark plasma sintering (SPS) is preferred over conventional sintering (CS), HIP or hot pressing (HP), as it produces a fine-grained microstructure [19]. Grain refinement in MAX phase ceramics might be an effective means of fabricating radiation-tolerant

materials, since grain boundaries have been shown to act as potent 'sinks' for radiation-induced defects [20].

This study focuses on the synthesis of Ti_3SnC_2 and two new MAX phases, Zr_3SnC_2 and Hf_3SnC_2, employing reactive SPS as the fast sintering technique of choice. The effect of adding Fe, Co or Ni to the starting powder is investigated and a comparison is made with the undoped ternary systems.

Materials and Methods

First, the powders were mixed in an elemental ratio M:Sn:C:Z = 3:1:2:0.6, where M corresponds to TiH_2, ZrH_2 or HfH_2, and Z to Fe, Co or Ni. This ratio corresponds to a targeted 10 at% of additive 'Z' in the overall 312 starting stoichiometry, since Ouabadi et al. reported a maximum Ti_3SnC_2 content for the 10 at% Fe addition [15]. The produced ceramics are henceforth labeled in this text as 'M312+Z'. The starting powders used in this work for MAX phase synthesis are described in Table 1. As a reference, ceramics without additives (M:Sn:C ratio = 3:1:2) were prepared. The powder mixture was made in a polypropylene jar and homogeneously dry-mixed on a multidirectional mixer (type Turbula) in air for 24 h. The mixed powder was poured in a graphite die with inner diameter of 30 mm and pre-compacted at 50 MPa. The sintering cycle was programmed starting with a fast heating to 450°C in 40 s. An initial minimal load of 7 MPa was applied to ensure a good electrical contact. Subsequently, a pyrometer-controlled heating rate of 50°C/min was adopted to reach the sintering temperature. This temperature was set to 1200°C for all compositions. For the cases of M =Zr and Hf and Z = Ni, two additional SPS cycles were performed at 1300°C. At this temperature, the load was increased to 50 MPa during a dwell time of 10 min. During the whole SPS-cycle, a vacuum level of ~100 Pa was maintained inside the SPS furnace (FCT-Systeme, HP D 25, Frankenblick, Germany). The piston displacement and vacuum level were monitored during the thermal cycle. A detailed description of the SPS setup is presented elsewhere [21]. In order to verify certain steps in the reaction scheme, some interrupted sintering experiments were performed in which the heating cycle was abruptly stopped at 1000°C. An overview of all conducted SPS experiments is given in Table 2.

After demolding, the ceramic discs were sandblasted, and the top surfaces were ground to remove the carbide reaction layer formed in direct contact with the graphite punch. The presented X-ray diffraction (XRD) patterns were measured using Cu K_α radiation under a Bragg-Brentano geometry (Bruker D2). The diffractometer was operating at 30 kV and 10 mA at room temperature. The XRD patterns were measured from 5° to 75° 2θ with a step size of 0.01° 2θ and 0.5 s per step. The Materials Analysis Using Diffraction (MAUD) software was used to perform Rietveld refinement [22].

Scanning electron microscopy (SEM; XL30-FEG, FEI, The Netherlands) supported with an energy dispersive X-ray spectrometer (EDS; EDAX) was used for microstructural characterization. Electron probe microanalysis (EPMA; JXA-8530F, JEOL Ltd., Japan) was used to map the elemental distribution

in the produced ceramics by means of wavelength dispersive X-ray spectroscopy (WDS), using a beam current of 15 nA and an accelerating voltage of 15 kV.

Table 1: Starting powders for MAX phase synthesis.

Powder	Supplier	Size	Purity
TiH_2	Rockwood Lithium, grade VM	< 2 µm	> 99 wt%
ZrH_2	Rockwood Lithium, grade G	< 6 µm	> 98 wt%
HfH_2	Rockwood Lithium, grade PS	< 36 µm	> 98 wt%
Sn	AEE, grade Sn-101	< 5 µm	> 99 wt%
C	Asbury Graphite Mills, US	< 5 µm	> 99 wt%
Fe	BASF, Carbonyl	< 10 µm	> 99 wt%
Co	Umicore, HMP	< 0.5 µm	> 99 wt%
Ni	AEE, grade Ni-110	4-8 µm	> 99 wt%

Table 2: Overview of the SPS experiments performed.

M	Sn	C	Z	Temperature (°C)	Interrupted or complete sintering cycle
3 Zr/Hf/Ti	1	2	0.6 Fe/Co/Ni	1200	Complete
3 Zr/Hf/Ti	1	2	/	1200	Complete
3 Zr/Hf	1	2	0.6 Ni	1300	Complete
3 Zr/Hf/Ti	1	2	0.6 Ni	1000	Interrupted
3 Zr	1	2	0.6 Co	1000	Interrupted

Results

The XRD patterns of the ceramics SPS at 1200°C are shown in Figure 1 and their phase assemblies are given in Table 3, where MAX phases are indicated in bold characters. In general, the addition of Fe, Co or Ni triggered the formation of 312-stackings, while suppressing the formation of 211-stackings. For the ceramics without Z-element, only the 211 structure was observed. Only in the case of Hf312 with Ni addition, a mixture of 312 and 211 phases was formed. The lattice parameters (LPs) *a* and *c* for all observed 312 phases were calculated using the Rietveld refinement method. The results are summarized in Table 4, where the uncertainty is typically of the order of 2×10^{-4} Å and 10^{-3} Å for the *a* and *c* LPs, respectively. The LPs for Ti_3SnC_2 with Fe as additive are in good agreement with those reported by Dubois et al. [14].

For a given M-element, the lattice parameters are not significantly affected by the Z-element additive, remaining within the range of uncertainty. Two reasons for this observation can be proposed: (a) if the

Z-element is present in the MAX phase structure, its quantity is very limited (> 0.1 wt%) as it could not be determined unambiguously with the used techniques (EDS and WDS) and (b) the Fe, Co and Ni atomic radii are similar. The LP variation for the three M-elements is consistent with the ranking of the atomic radii (Zr > Hf > Ti) [23] and is in agreement with the trend in LPs for other $M_{n+1}AX_n$ phases with M = Ti, Zr and Hf, for fixed A and X elements [24].

Looking at the other phases, the binary carbides TiC, ZrC and HfC were always present. Apart from the binary carbides, several intermetallic phases formed, the type of which was mainly determined by the Z-element additive and to a less extent by the M-element. For the ceramics without Fe, Co or Ni addition, M_5Sn_3 is observed in all three systems. For Zr and Hf, this is the most stable intermetallic compound, as reflected by a high melting point, T_m, i.e., T_m = 1988°C for Zr_5Sn_3 and T_m = 1971°C for Hf_5Sn_3. In the Hf system, some unreacted Hf was detected. In the Ti system, apart from Ti_5Sn_3 (T_m = 1510°C), Ti_3Sn was observed, which is the highest melting point intermetallic (T_m = 1670°C) in the Ti-Sn system.

For the Fe-doped materials, a trace amount of a binary intermetallic is observed, i.e., FeSn for M = Ti and Hf, and $FeSn_2$ for M = Zr. Both phases must have formed during cooling, as all Sn-rich (≥ 50 at%) phases in the Fe-Sn phase diagram are molten above 1130°C. By adding Co to the ternary systems, full-Heusler alloys with an overall formula of Co_2MSn are formed [25]. The Ni_2TiSn intermetallic also formed in the case of Ti_3SnC_2+Ni, together with a small amount of NiTi. The Ni-containing Zr- and Hf-based ceramics produced at 1200°C contained half-Heusler alloys with the NiSnZr and NiSnHf stoichiometries. These intermetallics are brittle stoichiometric compounds [26]. The reason for the difference between Ti and Zr/Hf with Ni as additive is most probably the difference in the melting point of the half-Heusler alloys: NiSnTi melts below the sintering temperature (T_m = 1180°C), whereas NiSnZr and NiSnHf are solid at 1200°C (T_m is 1435°C and 1487°C, respectively) [27].

In order to verify this effect of temperature in the case of Ni, two additional ceramics for M = Zr and Hf were made at 1300°C and three SPS cycles were interrupted at 1000°C for the different M elements. The X-ray patterns are shown in Figure 2. The quantified phase content of the ceramics synthesized at 1300°C is also included in Table 3. At 1300°C, full-Heusler alloys (Ni_2ZrSn/Ni_2HfSn) are present together with the half-Heusler alloys (NiZrSn/NiHfSn), the binary carbide phase (ZrC/HfC) and the 312 MAX phase. No 211 phase was detected for the case of Hf and for both cases, Zr and Hf, an increase in MAX phase content was observed. It illustrates that for these MAX phases the optimal synthesis temperature does not entirely depend on the ternary carbide phase but also partially on the additives and the secondary phases. As full-Heusler alloys contain less Sn than half-Heusler alloys, it can be assumed that the additional Sn is accommodated in the MAX phases. This can explain the higher 312-content at 1300°C for Zr and Hf. For the case of Ti, only Ni_2TiSn is present at 1200°C which indicates already a full conversion of the half- to full-Heusler alloy. It is possible that a higher temperature might even further increase the MAX phase content for Zr and Hf up to the level of a full conversion of the half- to full-Heusler alloy, but a full optimization of the synthesis process is beyond the scope of this study.

Another illustration of the difference between Ti and Zr/Hf for Z = Ni is the phase assembly at 1000°C. Due to the nature of the interrupted experiment, the system is not in thermodynamic equilibrium. Several phases were detected in all three materials of which the main ones are identified in Figure 2. However most relevant for this comparison is the fact that one can clearly identify the peaks of 312 phase in Ti312 + Ni material, whereas there is no sign of this MAX phase for Zr and Hf which requires a higher temperature to form. This fact is agreement with the observations stated above.

Table 3: Phase assembly of the ceramics, as determined by XRD. MAX phases are indicated in bold characters. The error in the quantification is in the range of ±1 wt%.

M	Z	T (°C)	Phase content (in wt%)
Ti	/	1200	**37 Ti_2SnC**, 36 TiC, 18 Ti_5Sn_3, 9 Ti_3Sn
	Fe	1200	**66 Ti_3SnC_2**, 30 TiC, 4 FeSn
	Co	1200	43 TiC, **38 Ti_3SnC_2**, 13 Co_2TiSn, 6 Sn
	Ni	1200	**63 Ti_3SnC_2**, 25 TiC, 8 Ni_2TiSn, 4 NiTi
Zr	/	1200	42 Zr_5Sn_3, 40 ZrC, **18 Zr_2SnC**
	Fe	1200	**64 Zr_3SnC_2**, 32 ZrC, 4 $FeSn_2$
	Co	1200	**43 Zr_3SnC_2**, 39 ZrC, 18 Co_2ZrSn
	Ni	1200	**36 Zr_3SnC_2**, 34 ZrC, 30 NiSnZr
		1300	**44 Zr_3SnC_2**, 30 ZrC, 15 NiSnZr, 11 Ni_2SnZr
Hf	/	1200	35 Hf_5Sn_3, 32 HfC, **26 Hf_2SnC**, 7 Hf
	Fe	1200	**66 Hf_3SnC_2**, 31 HfC, 3 FeSn
	Co	1200	**56 Hf_3SnC_2**, 31 HfC, 13 Co_2SnHf
	Ni	1200	41 HfC, **29 Hf_3SnC_2**, **11 Hf_2SnC**, 19 NiSnHf
		1300	**45 Hf_3SnC_2**, 35 HfC, 12 NiSnHf, 8 Ni_2SnHf

Table 4: Lattice parameters *a* and *c* of the M_3SnC_2 structure, as a function of Fe, Co or Ni addition. The uncertainty on the experimental LP values is in the range of ± 10^{-3} Å.

	Z	Fe		Co		Ni	
M	***Exp./Ref.****	*a* (Å)	*c* (Å)	*a* (Å)	*c* (Å)	*a* (Å)	*c* (Å)
Ti	*Exp.*	3.1341(2)	18.641(1)	3.1352(2)	18.638(1)	3.1307(2)	18.650(1)
	Ref. [14]	3.1366(2)	18.650(2)	/	/	/	/
Zr	*Exp.*	3.3585(2)	19.876(1)	3.3604(2)	19.888(1)	3.3610(2)	19.895(1)
Hf	*Exp.*	3.3162(2)	19.611(1)	3.3185(2)	19.616(1)	3.3154(2)	19.615(1)

***** *Exp.*: experimentally determined in this work; *Ref.*: reference value given in [14].

In general, the analysis of the phase assembly of the produced ceramics shows that the M-element has a minor influence on the type of formed phases (Table 3). This is associated with the chemical similarity between Ti, Zr and Hf, which is clearly evident from the periodic table of elements.

The microstructures of the M_3SnC_2+Fe materials produced at 1200°C are presented in Figure 3. The elongated MAX phase grains can easily be identified as the main constituents. The binary carbides are confined between the MAX phase grain clusters. The grain size of the binary carbides is M-element specific and ranges from micrometric ZrC over sub-micrometric TiC to nanometric HfC. The binary carbides are embedded in a brittle Fe_xSn_y intermetallic matrix. This is illustrated in Figure 4, which presents the elemental mapping for the Fe-doped Zr_3SnC_2 and Hf_3SnC_2 ceramics. The distribution of Fe is most interesting, because Fe is not considered as an M, A or X element in MAX phases. The MAX phase grain areas (A and B mark Zr_3SnC_2 and Hf_3SnC_2 grains, respectively) contain no Fe (detection limit is < 0.1 wt%), whereas the higher Fe contents are clearly overlapping with the areas occupied by Sn-rich intermetallics. This observation is consistent with the unaffected MAX phase lattice parameters for different Z-elements.

The effect of the Fe, Ni and Co additives on the microstructure is illustrated in Figure 5 for the Zr_3SnC_2+Z case. The ceramics with Fe, Co or Ni addition (Figure 5b-d) are fully densified and Zr_3SnC_2 MAX phase grains can be clearly distinguished. The Fe-containing material has relatively large Zr_3SnC_2 and ZrC grains, compared to its Co- and Ni-containing counterparts. Whereas very fine-grained $FeSn_2$ is present at grain boundaries and triple points in the Fe-doped ceramic, Co_2SnZr and NiSnZr are present as relatively large separate 'islands' in the Co- and Ni-doped materials. A brighter phase, not detected by XRD, is also observed between the carbide grains in the Co- and Ni-containing materials. This phase contained mainly Co (or Ni) and Sn, according to the EPMA results, and was labelled as Co_xSn_y (Figure 5c) and Ni_xSn_y (Figure 5d), respectively.

The ceramic containing only Zr, Sn and C (Figure 5a) has a completely different appearance. First, the material is not fully densified and pores can be distinguished between the various phases that correspond to those identified by XRD (Table 3) together with some unreacted C. This structure resembles strongly the one observed during the formation of Ti_2SnC, where MAX phase formation took place between the TiC binary carbide and a Sn-containing intermetallic [19, 28].

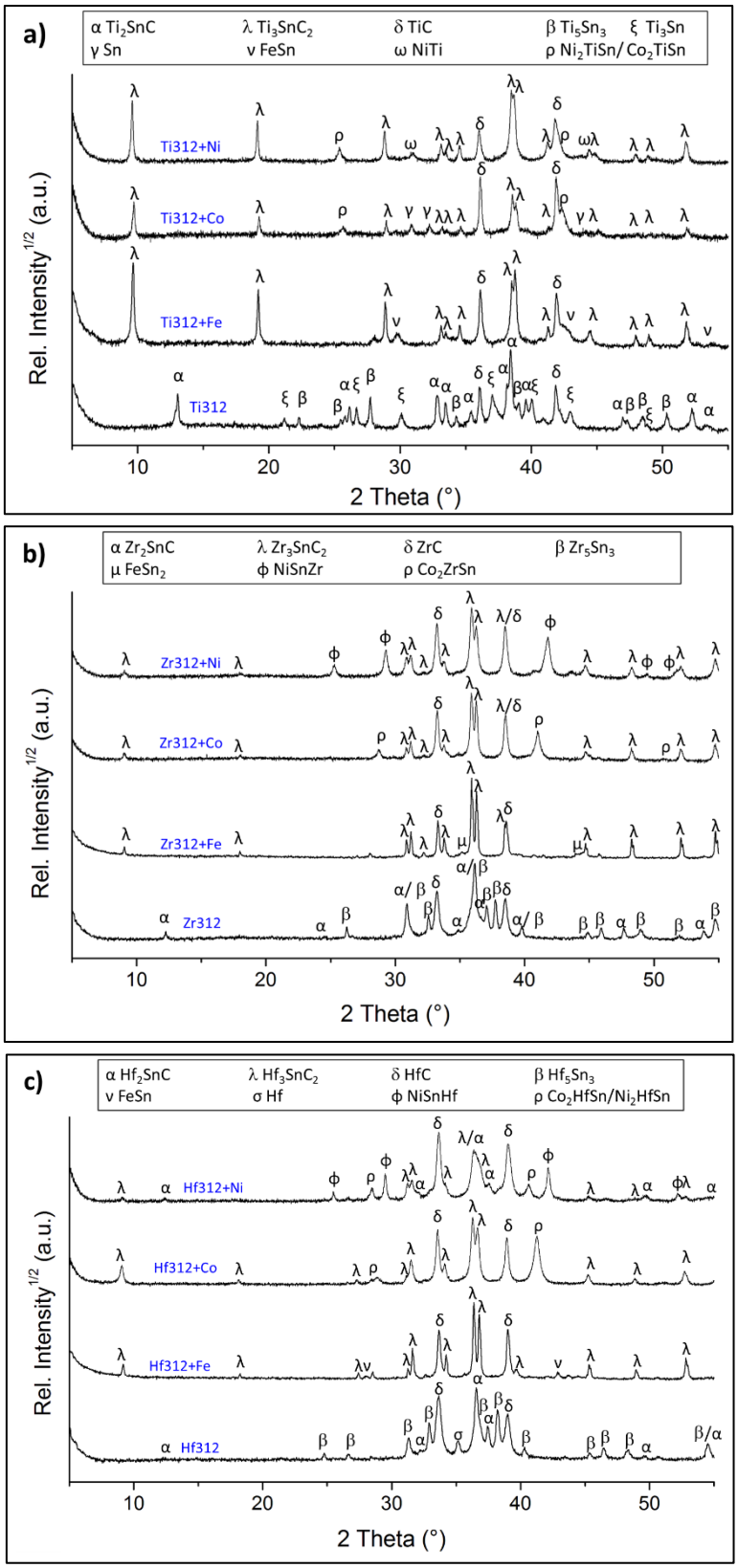

Figure 1: XRD patterns of the ceramics produced at 1200°C with (a) Ti312+Z (Ti_3SnC_2 + 0.6Z), (b) Zr312+Z (Zr_3SnC_2 + 0.6 Z) and (c) Hf312+Z (Hf_3SnC_2 + 0.6 Z), with Z = Fe, Co or Ni.

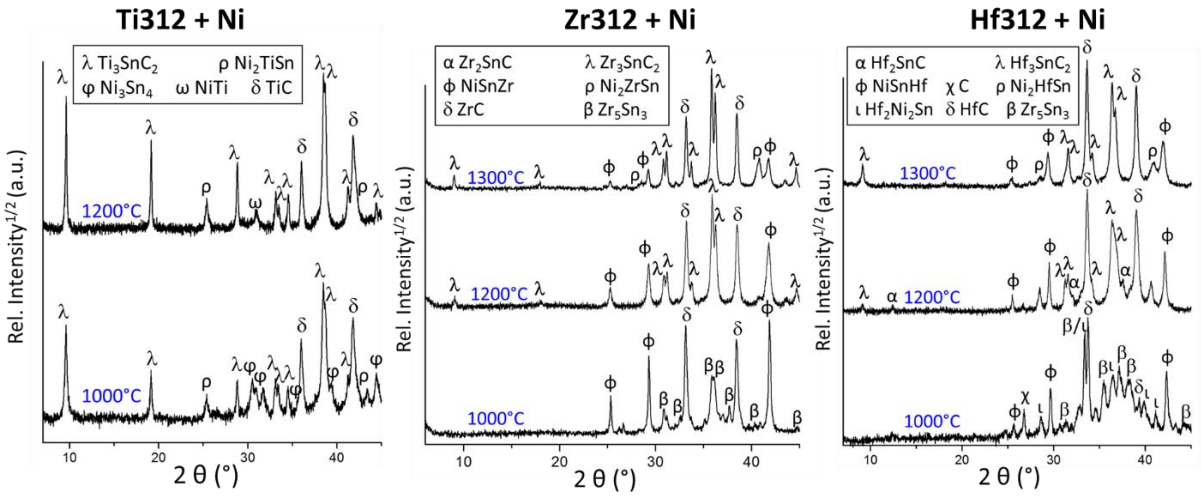

Figure 2: XRD patterns of M_3SnC_2 + 0.6 Ni for different temperatures. The 1000°C patterns were obtained from interrupted SPS cycles.

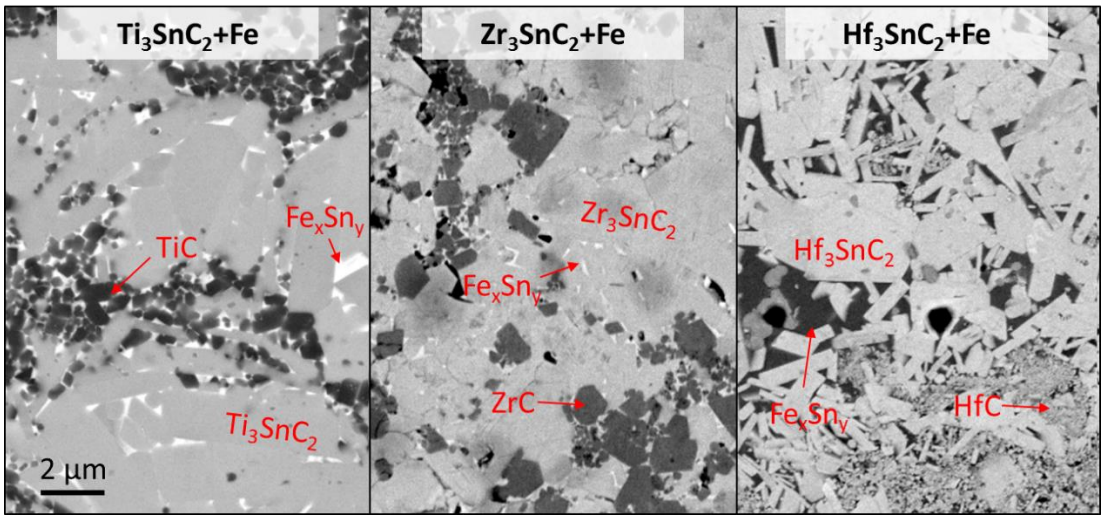

Figure 3: Backscattered electron (BSE) micrographs of the M_3SnC_2+Fe ceramics produced at 1200°C.

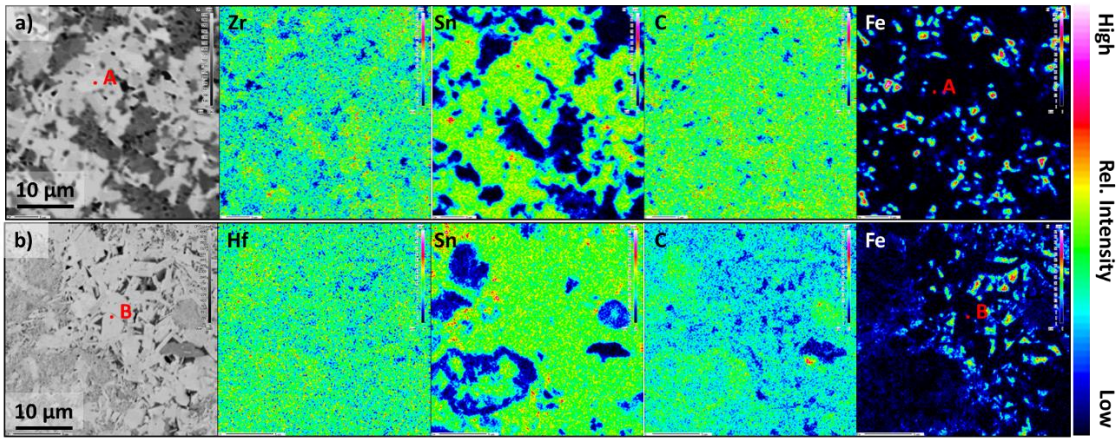

Figure 4: Elemental mapping for (a) Zr_3SnC_2+Fe and (b) Hf_3SnC_2+Fe both produced at 1200°C. Points A and B correspond to a Zr_3SnC_2 and a Hf_3SnC_2 grain, respectively.

Discussion

The experimental evidence shows that the addition of 10 at % Fe, Co or Ni enhances and changes the reaction scheme for the formation of MAX phases in the studied systems. The effect of Fe on the formation mechanism of Ti_3SnC_2 was studied by Ouabadi et al. [15]. Despite the fact that no Fe was observed inside the MAX phase lamellae, the additive is thought to play a key role in the formation of the 312 stacking. In fact, it was proposed that Ti_3SnC_2 forms via a dissolution-diffusion-precipitation mechanism in a molten Fe_xSn_y phase [15]. This suggestion still holds for the observed phase formation in the present work. Liquid Fe_xSn_y was present at 1200°C (solidified as $FeSn_2$ or FeSn during cooling) in the three Fe-containing ceramics, promoting densification and the ongoing reactions. A similar mechanism can be proposed for Co and Ni, where the 312 MAX phase precipitated from a molten intermetallic phase, which is still observed at grain boundaries. This liquid phase is most likely also responsible for the improved densification and reaction rate. Furthermore, it should be mentioned that elements from groups 8, 9 and 10 (Group VIII in the old notation) in the periodic table (i.e., Fe, Co and Ni) are known to enhance the sinterability of transition metals and their carbides by reducing the activation energy for diffusion in the system (i.e., addition of Ni in Ag-WC) [29, 30].

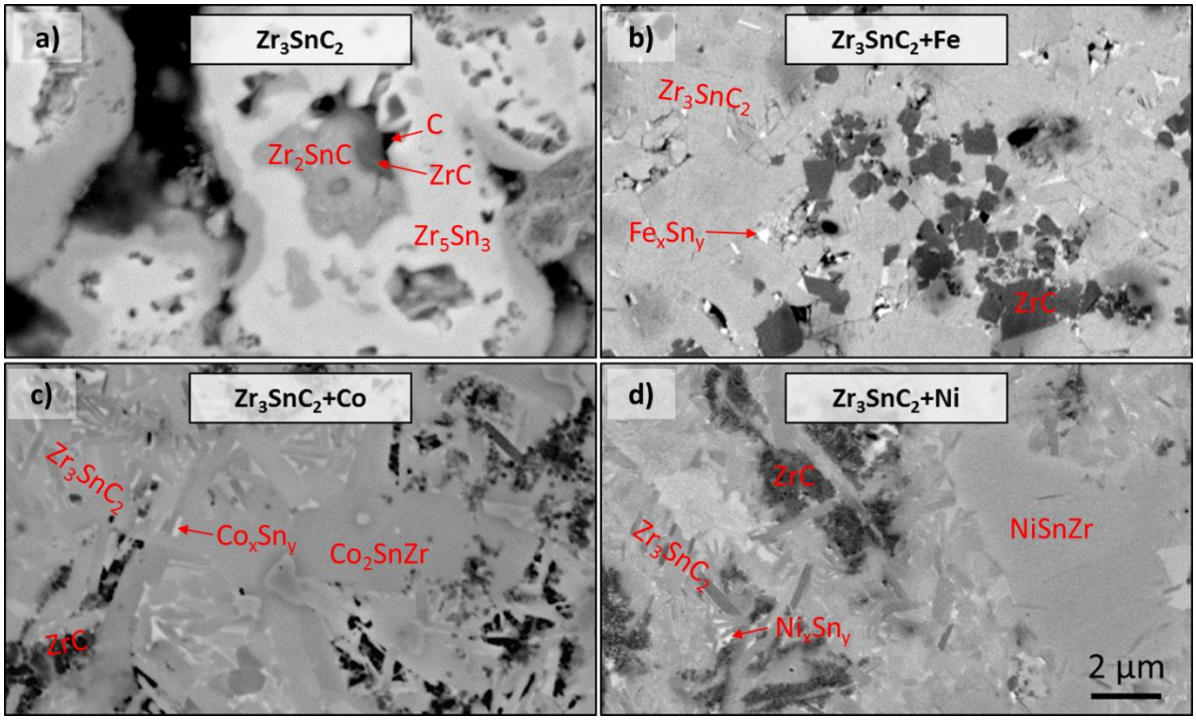

Figure 5: Influence of the additive on the microstructure of Zr_3SnC_2+Z ceramics produced at 1200°C: without additive (a) and with Z = Fe (b), Co (c) and Ni (d).

What remains puzzling is why additives like Fe, Co or Ni change the atomic stacking of the MAX phases without being present in the crystal structure. Co and Ni have never been observed as MAX phase constituent elements. Fe has not been considered as solely M- or A-element. However, Hf_2SC has been considered as a quaternary compound, probably containing some Fe [31, 32]. More recently, a study on

(Cr_{2-x},M_x)GeC stated that Cr could be partially replaced by Fe [33]. However, the observed Hf_2SC and (Cr_{2-x},M_x)GeC structures were both 211-type MAX phases, whereas 312-type MAX phases were observed in the present work.

A critical point is the transition from the 211 to the 312 structure. It was clearly shown in the work of Ouabadi et al. that Ti_2SnC forms first at lower temperatures (around 1000°C), while Ti_3SnC_2 forms only in a later stage, at higher temperatures (> 1100°C) [15]. Two reactions were proposed for the formation of the 312-type MAX phase [15]:

$$Ti_5Sn_3 + 2\ TiC + 2\ Ti + 4C \rightarrow 3Ti_3SnC_2 \quad (1)$$

$$Ti_2SnC + TiC \rightarrow Ti_3SnC_2 \quad (2)$$

Due to the high degree of chemical similarity with the materials studied in this work, it is reasonable to assume that the M_2SnC phases formed first, and the conversion to M_3SnC_2 took place upon further heating. Experimental evidence was obtained by performing interrupted SPS experiments for Zr312 + M, where the sintering cycle was abruptly stopped at 1000°C. Figure 6 shows a comparison of three diffractograms where the main constituting phases are identified. For the case of Fe and Co, a Zr_2SnC fraction is clearly present, whereas there is no sign of any MAX phase with Ni at 1000°C. It can be speculated that the presence of Ni increases the temperature needed to synthesise Zr_2SnC, similar as observed and described above for Zr_3SnC_2 and Hf_3SnC_2. The reason for this delayed reaction is unclear. However, the presence of a 211 fraction at 1200°C for Hf_3SnC_2 + Ni (see Fig. 2 and Table 3) illustrates the formation of M_2SnC as intermediate reaction product in the Ni-containing systems.

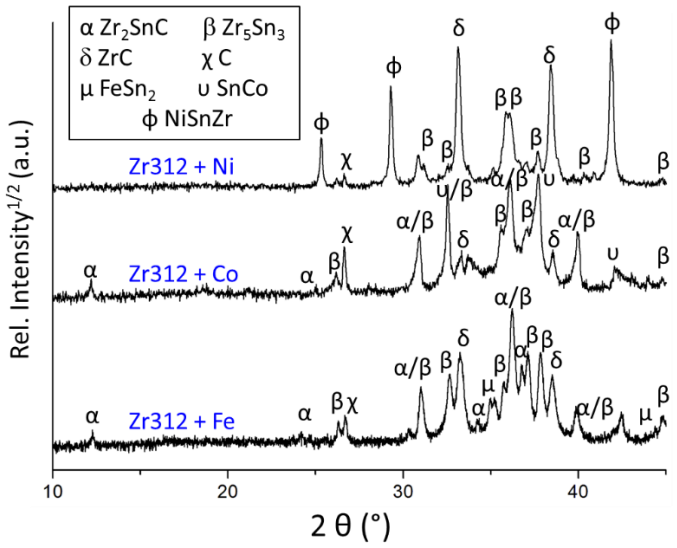

Figure 6: XRD patterns of material with Zr_3SnC_2 + 0.6 M composition produced by interrupted SPS cycles at 1000°C.

From the presented data it is clear that the presence of the Z-element is indispensable to facilitate the formation of M_3SnC_2. It however remains a curious fact that what was initially introduced as an impurity, i.e. iron form the steel HIP capsule [14], can modify the atomic stacking in the MAX phase structure. Similarly, it has been reported for other MAX phase systems that the presence of impurities in the starting powder can help the nucleation and growth of these ternary carbides [34]. Moreover it was already mentioned by Nowotny that 'minute amounts of other non-metal elements (N, O, H etc.) are sometimes able to stabilize carbide structures, which either do not exist or cannot be prepared in the absence of these impurities' [32]. In the present M_3SnC_2 + Z case, there is no evidence for the incorporation of the Z element in the MAX structure, as can happen for Si or for light element impurities such as N, O or H. In order to clarify the role of the Z-element in the formation of M_3SnC_2 an alternative explanation is proposed. The addition of Fe and Ni has been reported to significantly enhance the wettability of TiC by non-reactive liquid metals [35]. This enhanced reactivity was explained by the possibility for Ni and Fe to dissolve C, whereas the tested liquids, i.e. Au, Ag and Sn show negligible solubility for carbon [35, 36]. A similar reasoning can be applied to Co which has also a certain solubility for C. Hence it can be assumed that due to this enhanced wettability, reactions (1) and (2) can take place where the liquid Z_xSn_y facilitates C-transport between the intermetallic and MC (reaction (1)) or between M_2SnC and MC (reaction (2)) which is not possible in pure Sn. The latter reaction can, on an atomic level, be expressed as a rearrangement of Sn and C where the amount of M-atoms stay net the same, the amount of Sn decreases and the amount of C increases:

$$3\ M_2SnC + C + (Z_xSn_y)_{liq} \rightarrow 2\ M_3SnC_2 + (Z_xSn_{y+1})_{liq} \qquad (3)$$

This reaction presents Sn as most mobile element in M_2SnC which is in agreement with most observed MAX phase transitions including the synthesis method of the new Ti_3AuC_2 [12]. Moreover the idea of the outward diffusion of the A-element during the transition is supported by the atomic configuration in the 211-to-312-transition zone observed in the Hf-Al-C system [37].

In terms of its effectiveness as 312 MAX phase 'catalyst' – M_3SnC_2 formed per Z – Fe is the most effective additive when compared to Co and Ni. This statement is based on the quantified phase assembly (Table 3), where the M_3SnC_2 content is substantially higher in the presence of Fe. This is further supported by the microstructural analysis (Figure 5): the MAX phase lamellae are the main phase present in case of the Fe addition (Figure 5b) whereas they are smaller and less present after the Co or Ni addition (Figure 5c-d). An explanation for this difference can be found in the fact that Co and Ni are mainly contained in the brittle (half-)Heusler phases that remain in the solid state during processing and do not contribute to MAX phase formation.

Overall, reaction (3) is, to our understanding, the best way to express the participation of the Z element, which is essential for the reaction to occur without being present in the 312 MAX phase structure. An unfortunate side-effect of this reaction is that it seems impossible to synthesize phase-pure M_3SnC_2

materials. Nevertheless, it is an intriguing feature that a (small) amount of an element that does not result in MAX phase formation can trigger a change in the atomic stacking of the MAX phase structure.

Conclusions

10 at% Fe, Co and Ni (the Z-elements) were added to a powder mixture of $3MH_2$: Sn : 2C, with M = Ti, Zr or Hf, in order to study their effect on the phase assembly and microstructure after reactive SPS for 10 min at 1200°C. The additives promoted densification and MAX phase formation. The Z-element dopant resulted in 312-type MAX phase formation, whereas the non-doped reference materials only contained limited (< 40 wt%) amounts of the 211-structure. Binary MC carbides were always present in the produced ceramics, along with Sn-containing intermetallics, the type of which mainly depended on the Z-element.

Following this approach, two new MAX phases were discovered, i.e., Zr_3SnC_2 and Hf_3SnC_2. The *a* and *c* lattice parameters of all 312 MAX phases were determined by XRD in combination with Rietveld refinement. The lattice parameters were not significantly influenced by the type of additive (Fe, Co or Ni). Despite the need for a Z-element to form the M_3SnC_2 structure, no Z-element could be detected in the MAX phase lamellae with the employed detection techniques (< 0.1 wt%). The formation mechanism of this MAX phase type was discussed and could be related to the enhanced mass transport and solution-precipitation enabled by a liquid Z_xSn_y phase. Overall, Fe addition was more efficient in terms of MAX phase yield (M_3SnC_2 > 60 wt%) than Ni or Co addition, due to the formation of thermally-stable Heusler alloy phases (Z_2MSn or ZMSn) with Co and Ni.

Acknowledgements

This research was partly funded by PhD grant No. 131081 of the Agency for Innovation by Science and Technology (IWT), Flanders, Belgium, partly by the European Atomic Energy Community's (Euratom) Seventh Framework Programme FP7/2007-2013 under grant agreement No. 604862 (FP7 MatISSE), and falls within the framework of the EERA (European Energy Research Alliance) Joint Programme on Nuclear Materials (JPNM). The University of Poitiers, France, is gratefully acknowledged for funding a Visiting Professor position for K. Lambrinou.

References

[1] W. Jeitschko, H. Nowotny, and F. Benesovsky, "Kohlenstoffhaltige ternäre Phasen (H-Phase)," *Monatshefte für Chemie,* vol. 94, pp. 672 - 676, 1963

[2] W. Jeitschko, H. Nowotny, and F. Benesovsky, "Carbides of formula T_2MC," *Journal of the Less Common Metals,* vol. 7, pp. 133-138, 1964.

[3] M. W. Barsoum, "The $M_{n+1}AX_n$ phases: A new class of solids: Thermodynamically stable nanolaminates," *Progress in Solid State Chemistry,* vol. 28, pp. 201-281, 2000.

[4] M. W. Barsoum and T. El-Raghy, "Synthesis and Characterization of a Remarkable Ceramic: Ti_3SiC_2," *Journal of the American Ceramic Society,* vol. 79, pp. 1953-1956, 1996.

[5] M. W. Barsoum, *MAX Phases: Properties of Machinable Ternary Carbides and Nitrides*: Wiley-VCH Verlag GmbH & Co., 2013.

[6] M. Naguib, G. W. Bentzel, J. Shah, J. Halim, E. N. Caspi, J. Lu*, et al.*, "New Solid Solution MAX Phases: $(Ti_{0.5}, V_{0.5})_3AlC_2$, $(Nb_{0.5}, V_{0.5})_2AlC$, $(Nb_{0.5}, V_{0.5})_4AlC_3$ and $(Nb_{0.8}, Zr_{0.2})_2AlC$," *Materials Research Letters,* vol. 2, pp. 233-240, 2014.

[7] E. N. Caspi, P. Chartier, F. Porcher, F. Damay, and T. Cabioc'h, "Ordering of (Cr,V) Layers in Nanolamellar $(Cr_{0.5}V_{0.5})_{n+1}AlC_n$ Compounds," *Materials Research Letters,* vol. 3, pp. 100-106, 2015.

[8] A. S. Ingason, A. Petruhins, M. Dahlqvist, F. Magnus, A. Mockute, B. Alling*, et al.*, "A Nanolaminated Magnetic Phase: Mn_2GaC," *Materials Research Letters,* vol. 2, pp. 89-93, 2014.

[9] T. Lapauw, K. Lambrinou, T. Cabioc'h, J. Halim, J. Lu, A. Pesach*, et al.*, "Synthesis of the new MAX phase Zr_2AlC," *Journal of the European Ceramic Society,* vol. 36, pp. 1847-1853, 2016.

[10] T. Lapauw, J. Halim, J. Lu, T. Cabioc'h, L. Hultman, M. W. Barsoum*, et al.*, "Synthesis of the novel Zr_3AlC_2 MAX phase," *Journal of the European Ceramic Society,* vol. 36, pp. 943-947, 2016.

[11] T. Lapauw, D. Tytko, K. Vanmeensel, S. Huang, P.-P. Choi, D. Raabe*, et al.*, "$(Nb_x, Zr_{1-x})_4AlC_3$ MAX Phase Solid Solutions: Processing, Mechanical Properties, and Density Functional Theory Calculations," *Inorganic Chemistry,* vol. 55, pp. 5445-5452, 2016.

[12] H. Fashandi, M. Dahlqvist, J. Lu, J. Palisaitis, S. I. Simak, I. A. Abrikosov*, et al.*, "Synthesis of Ti_3AuC_2, $Ti_3Au_2C_2$ and Ti_3IrC_2 by noble metal substitution reaction in Ti_3SiC_2 for high-temperature-stable Ohmic contacts to SiC," *Nat Mater,* vol. advance online publication, online 2017.

[13] D. T. Cuskelly, E. R. Richards, E. H. Kisi, and V. J. Keast, "Ti_3GaC_2 and Ti_3InC_2: First bulk synthesis, DFT stability calculations and structural systematics," *Journal of Solid State Chemistry,* vol. 230, pp. 418-425, 2015.

[14] S. Dubois, T. Cabioc'h, P. Chartier, V. Gauthier, and M. Jaouen, "A new ternary nanolaminate carbide: Ti3SnC2," *Journal of the American Ceramic Society,* vol. 90, pp. 2642-2644, 2007.

[15] N. Ouabadi, V. Gauthier-Brunet, T. Cabioc'h, G.-P. Bei, and S. Dubois, "Formation Mechanisms of Ti_3SnC_2 Nanolaminate Carbide Using Fe as Additive," *Journal of the American Ceramic Society,* vol. 96, pp. 3239-3242, 2013.

[16] T. El-Raghy, S. Chakraborty, and M. W. Barsoum, "Synthesis and characterization of Hf_2PbC, Zr_2PbC and M_2SnC (M=Ti, Hf, Nb or Zr)," *Journal of the European Ceramic Society,* vol. 20, pp. 2619-2625, 2000.

[17] W. Jeitschko, H. Nowotny, and F. Benesovsky, "Die H-Phasen Ti_2TlC, Ti_2PbC, Nb_2InC, Nb_2SnC und Ta_2GaC," *Monatshefte für Chemie und verwandte Teile anderer Wissenschaften,* vol. 95, pp. 431-435, 1964.

[18] S. Li, G. Bei, X. Chen, L. Zhang, Y. Zhou, M. Mačković*, et al.*, "Crack healing induced electrical and mechanical properties recovery in a Ti_2SnC ceramic," *Journal of the European Ceramic Society,* vol. 36, pp. 25-32, 2016.

[19] T. Lapauw, K. Vanmeensel, K. Lambrinou, and J. Vleugels, "Rapid synthesis and elastic properties of fine-grained Ti_2SnC produced by spark plasma sintering," *Journal of Alloys and Compounds,* vol. 631, pp. 72-76, 2015.

[20] D. J. Tallman, L. He, J. Gan, E. a. N. Caspi, E. N. Hoffman, and M. W. Barsoum, "Effects of neutron irradiation of Ti_3SiC_2 and Ti_3AlC_2 in the 121–1085 °C temperature range," *Journal of Nuclear Materials,* vol. 484, pp. 120-134, 2017.

[21] K. Vanmeensel, A. Laptev, J. Hennicke, J. Vleugels, and O. Van der Biest, "Modelling of the temperature distribution during field assisted sintering," *Acta Materialia,* vol. 53, pp. 4379-4388, Sep 2005.

[22] L. Lutterotti, S. Matthies, and H. Wenk, "MAUD: a friendly Java program for material analysis using diffraction," *Newsletter of the CPD,* vol. 21, pp. 14-15, 1999.

[23] J. C. Slater, "Atomic Radii in Crystals," *The Journal of Chemical Physics,* vol. 41, pp. 3199-3204, 1964.

[24] M. W. Barsoum, G. Yaroschuk, and S. Tyagi, "Fabrication and characterization of M2SnC (M = Ti, Zr, Hf and Nb)," *Scripta Materialia,* vol. 37, pp. 1583-1591, 1997.

[25] K. Endo, A. Shinogi, and I. Vincze, "Hyperfine Fields at Tin Site in Heusler Alloys: Co_2TiSn, Co_2ZrSn and Co_2HfSn," *Journal of the Physical Society of Japan,* vol. 40, pp. 674-678, 1976.

[26] G. Rogl, A. Grytsiv, M. Gürth, A. Tavassoli, C. Ebner, A. Wünschek*, et al.*, "Mechanical properties of half-Heusler alloys," *Acta Materialia,* vol. 107, pp. 178-195, 2016.

[27] D.-y. Jung, K. Kurosaki, C.-e. Kim, H. Muta, and S. Yamanaka, "Thermal expansion and melting temperature of the half-Heusler compounds: MNiSn (M = Ti, Zr, Hf)," *Journal of Alloys and Compounds,* vol. 489, pp. 328-331, 2010.

[28] Y. C. Zhou, H. Y. Dong, X. H. Wang, and C. K. Yan, "Preparation of Ti2SnC by solid-liquid reaction synthesis and simultaneous densification method," *Materials Research Innovations,* vol. 6, pp. 219-225, 2002.

[29] P. E. Zovas, R. M. German, K. S. Hwang, and C. J. Li, "Activated and Liquid-Phase Sintering—Progress and Problems," *JOM,* vol. 35, pp. 28-33, 1983.

[30] T. Mützel and B. Kempf, "Silver tungsten carbide contacts fork circuit breaker applications," in *2014 IEEE 60th Holm Conference on Electrical Contacts (Holm)*, 2014, pp. 1-7.

[31] H. Kudielka, *Z. Kristallogr. Kristallgeom. Kristallphys. Kristallchem.,* vol. 121, p. 165, 1965.

[32] H. Nowotny, "Crystal Chemistry of Complex Carbides and Related Compounds," *Angewandte Chemie International Edition in English,* vol. 11, pp. 906-915, 1972.

[33] S. Lin, Y. Huang, L. Zu, X. Kan, J. Lin, W. Song*, et al.*, "Alloying effects on structural, magnetic, and electrical/thermal transport properties in MAX-phase $Cr_{2-x}M_xGeC$ (M=Ti, V, Mn, Fe, and Mo)," *Journal of Alloys and Compounds,* vol. 680, pp. 452-461, 2016.

[34] E. Zapata-Solvas, S.-R. G. Christopoulos, N. Ni, D. C. Parfitt, D. Horlait, M. E. Fitzpatrick*, et al.*, "Experimental synthesis and density functional theory investigation of radiation tolerance of $Zr_3(Al_{1-x}Si_x)C_2$MAX phases," *Journal of the American Ceramic Society*, vol. 100, pp. 1377–1387, 2017.

[35] N. Frage, N. Froumin, and M. P. Dariel, "Wetting of TiC by non-reactive liquid metals," *Acta Materialia,* vol. 50, pp. 237-245, 2002.

[36] L. L. Oden and N. A. Gokcen, "Sn-C and Al-Sn-C phase diagrams and thermodynamic properties of C in the alloys: 1550 °C to 2300 °C," *Metallurgical Transactions B,* vol. 24, pp. 53-58, 1993.

[37] T. Lapauw, B. Tunca, T. Cabioc'h, J. Lu, P. O. Å. Persson, K. Lambrinou*, et al.*, "Synthesis of MAX Phases in the Hf–Al–C System," *Inorganic Chemistry,* vol. 55, pp. 10922-10927, 2016.